

¹ Meteorology Group, Departament de Física, Universitat de les Illes Balears, Palma de Mallorca, Spain

² Departament de Física i Enginyeria Nuclear, Universitat Politècnica de Catalunya, Vilanova i la Geltrú, Barcelona, Spain

Diagnosis and Numerical Simulation of a Torrential Precipitation Event in Catalonia (Spain)

C. Ramis¹, R. Romero¹, V. Homar¹, S. Alonso^{1, 2}, and M. Alarcón²

With 26 Figures

Received March 9, 1998

Revised June 17, 1998

Summary

A torrential precipitation event occurred in Catalonia (northeastern part of Spain) during 9 and 10 October 1994. More than 400 mm were registered in the south of Catalonia. A diagnostic study shows that most of the ingredients to produce heavy rain (large scale upward vertical motion, instability, high moisture content in all the troposphere) were present over the Spanish coast and western Mediterranean. Mesoscale triggering mechanisms have been associated with the orographic forcing, not only through physical lifting of moist air by the coastal mountains, but also by the redistribution of the surface pressure field induced by the Atlas and Pyrenees ranges. A numerical simulation of the event using a meso- β model has been performed. The model forecasts qualitatively well the rainfall distribution but underestimates the maximum rainfalls. The effects of the orography and the evaporation from the sea have been also studied. The simulations have shown that the action of the orography is decisive for the rainfall, pressure and wind distributions over the Spanish coast and the western Mediterranean. The isolated action of the evaporation turns to be much less important. However the combined effect of orography and evaporation is the most important factor in the areas where the greatest amount of rainfall occurred.

1. Introduction

During 9 and 10 October 1994 a heavy rain episode affected the eastern and north-eastern regions of Spain, from south Valencia to Catalonia (Fig. 1). The most important rainfall

occurred in the Alforja town (south Catalonia), where 450 mm fell (240 mm in an interval of about 2.5 hours, between 0500 and 0730 UTC on 10 October). In addition, very high amounts were also registered close to the coast as can be seen in Fig. 2. Floods were very important in Catalonia, producing damage on houses, farms, routs and railways. Moreover, 8 people lost their lives. Rainfalls continued over Valencia, Catalonia and Balearic Islands during 11, 12 and 13 October, but were more scattered and less intense.

The Spanish Mediterranean coastal region is affected by heavy rain several times during the year (Font, 1983), usually producing local flooding. There are examples of very extreme rainfalls, as the 800 mm recorded in 24 hours in Gandía (Valencia) on 3 November 1987. In a climatic study, Romero et al. (1998a) have shown that heavy precipitation events in that area tend to occur in autumn.

As a consequence of the social and economical impact produced by this kind of events, efforts have been conducted to study the meteorological situations in which heavy rain develops. For example, Llasat (1987) provides an extensive information on heavy rain events in north-eastern Spain; García-Dana et al. (1982), Ramis et al. (1994), Ramis et al. (1995) and Doswell et al. (1998) present diagnostic studies and Fernández

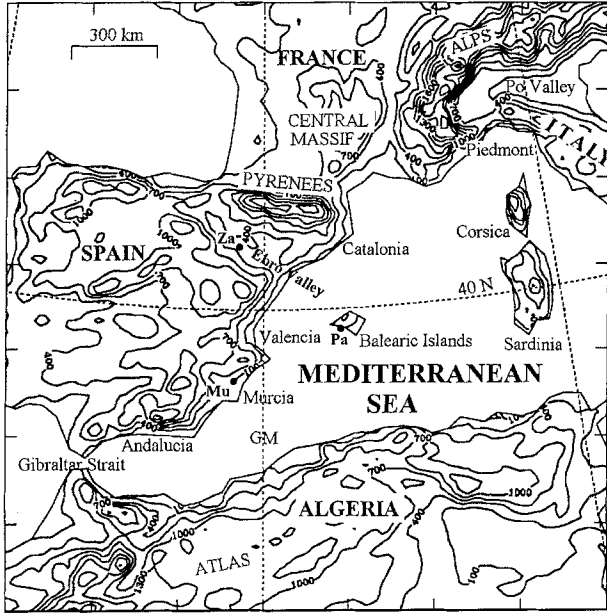


Fig. 1. The western Mediterranean region and its orography (contour interval is 300 m starting at 100 m). The sites mentioned in the text are indicated

et al. (1995), Romero et al. (1997), Romero et al. (1998b) and Codina et al. (1997) numerical simulations of heavy rain events in the Spanish Mediterranean region. Riosalido (1990) shows, from Meteosat pictures, that nearly stationary Mesoscale Convective Systems are responsible for most of the heavy precipitation events over eastern Spain.

The above referenced diagnostic studies show that some common features appear in the meteorological situations producing heavy rain: low level flow from the east or southeast and upper level flow from the southwest over the Spanish coast, and very warm and humid air over Mediterranean which is advected towards Spain. Moreover, moisture convergence in the lowest 1500 m and values of convective available potential energy (CAPE) greater than 2000 J kg^{-1} are usually found over the Mediterranean.

Numerical simulations of case studies have shown that mesoscale models normally underestimate the total rainfalls. These simulations have shown that coastal orography results a decisive factor in the localisation and spatial distribution of the rainfall (Romero et al., 1997; Romero et al., 1998b).

Codina et al. (1997) present a numerical simulation of the 9–10 October 1994 event

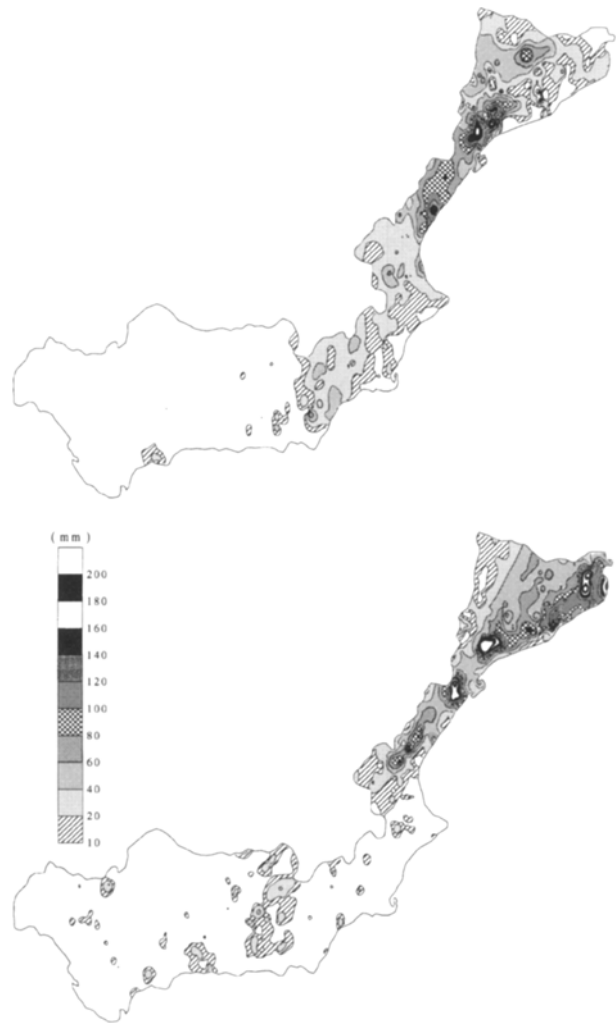


Fig. 2. Total precipitation (mm) in eastern and southern Spain. (a) from 07 UTC 9 October to 07 UTC 10 October 1994, (b) from 07 UTC 10 October to 07 UTC 11 October 1994

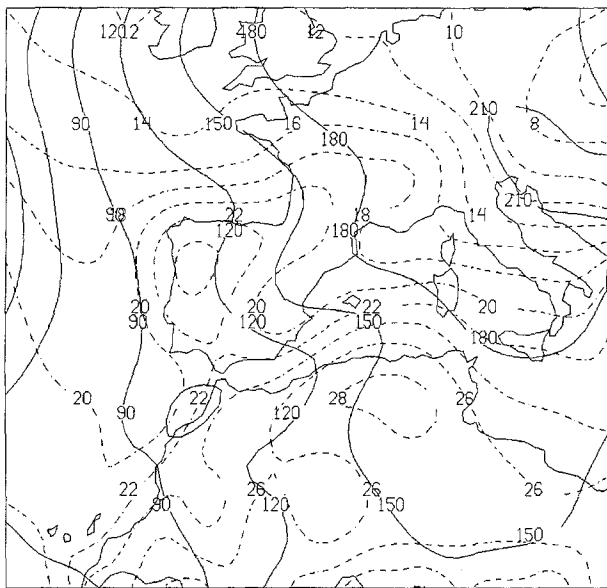
described before, using a nested numerical model (the MASS model). They show that the spatial structure of precipitation is correctly captured, but that the total amounts are underestimated. In this paper we present a diagnostic study and a numerical simulation of the same torrential event. In the diagnosis we are interested on the synoptic and mesoscale mechanisms responsible for the heavy precipitation. The numerical simulation has a double objective. First, we wish to continue testing the feasibility of mesoscale numerical modeling for the heavy rain problem. In second place, we are interested in studying the influence of orography and evaporation from the Mediterranean Sea in this kind of events. These

factors have been traditionally considered as the most important (Miró-Granada, 1974). The coastal orography of Spain can be an important physical lifting mechanism to develop convection, but the mountain ranges surrounding the western Mediterranean (Alps, Atlas, Pyrenees, etc.; see Fig. 1), can also interact with the synoptic flow and develop mesoscale pressure systems which can develop low levels convergences. In addition, the Mediterranean sea is still warm during autumn and evaporation may

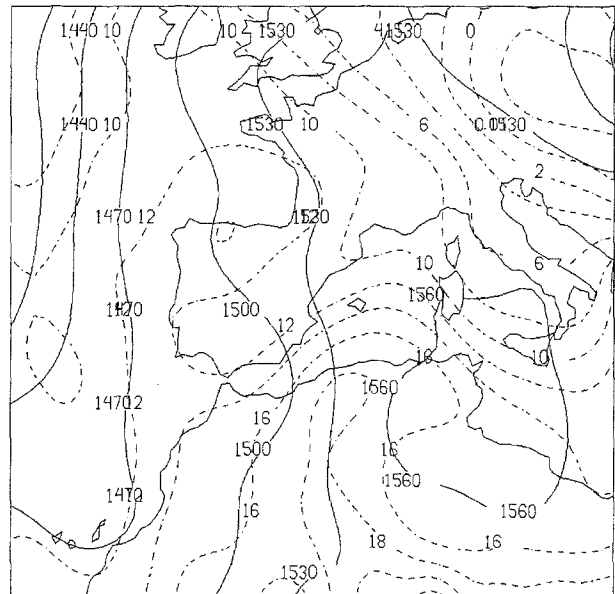
be intense, creating convective instability. The study of the effects of these two factors is done following the technique described by Stein and Alpert (1993).

2. Synoptic Overview

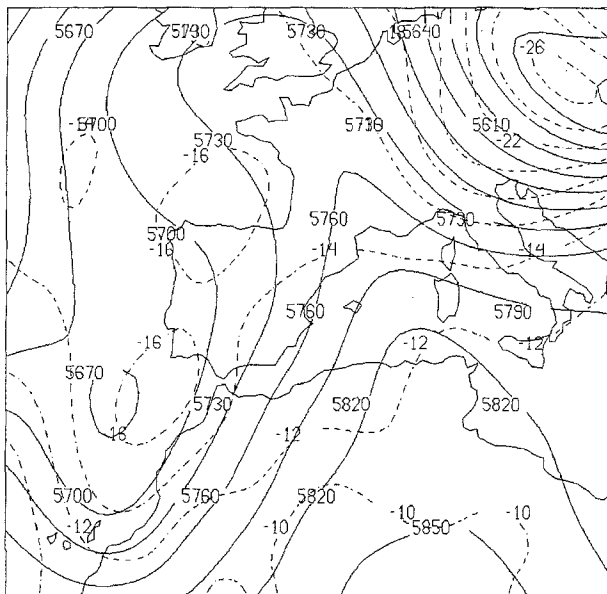
For shortness, we present only the meteorological situation at 12 UTC 9 October. Analyses come from ECMWF. The synoptic pattern at low levels (Fig. 3a) was characterised by an anti-



a



b



c

Fig. 3. Synoptic situation at 12 UTC 9 October 1994, showing height (gpm, continuous line) and temperature (°C, dashed line). (a) 1000 hPa, (b) 850 hPa, (c) 500 hPa

cyclone located north of Italy and extending towards north Africa. A low is located to the southwest of Spain. Over the western Mediterranean the flux is from the southeast as a consequence of a trough over the Algerian coast developed as the upper levels flux overcomes the Atlas (this will be shown in section 5). The wind is blowing and advecting warm air towards the Valencia and Murcia coasts. The same pattern can be identified at 850 hPa (Fig. 3b), but an important feature is a southerly low-level jet (LLJ) that points directly towards the Valencia and Murcia regions. At middle levels, (Fig. 3c), a trough, with a cold core, is located to the southwest of the Iberian peninsula producing south-southwest flux over the Spanish Mediterranean coast and northern Africa, in particular over the Atlas. A negative tilted ridge is located over the western Mediterranean extending

towards the British Isles. At upper levels, the pattern is very similar to 500 hPa but there is a jet streak from the southwest over Spain. It is interesting to note that warm air is present in all the troposphere over the western Mediterranean.

The synoptic situation evolved very slowly in the subsequent 18 hours (charts not shown). On 06 UTC 10 October, the European high pressure centre has reinforced slightly but remains stationary. The flux over the western Mediterranean is still from the east-southeast, but the low levels winds point towards the Catalonia and north Valencia regions. The LLJ at 850 hPa is also directed towards Catalonia producing warm advection. At 500 hPa, the trough has moved towards the east, being now negatively tilted. The ridge over the western Mediterranean only experiences a small displacement towards the

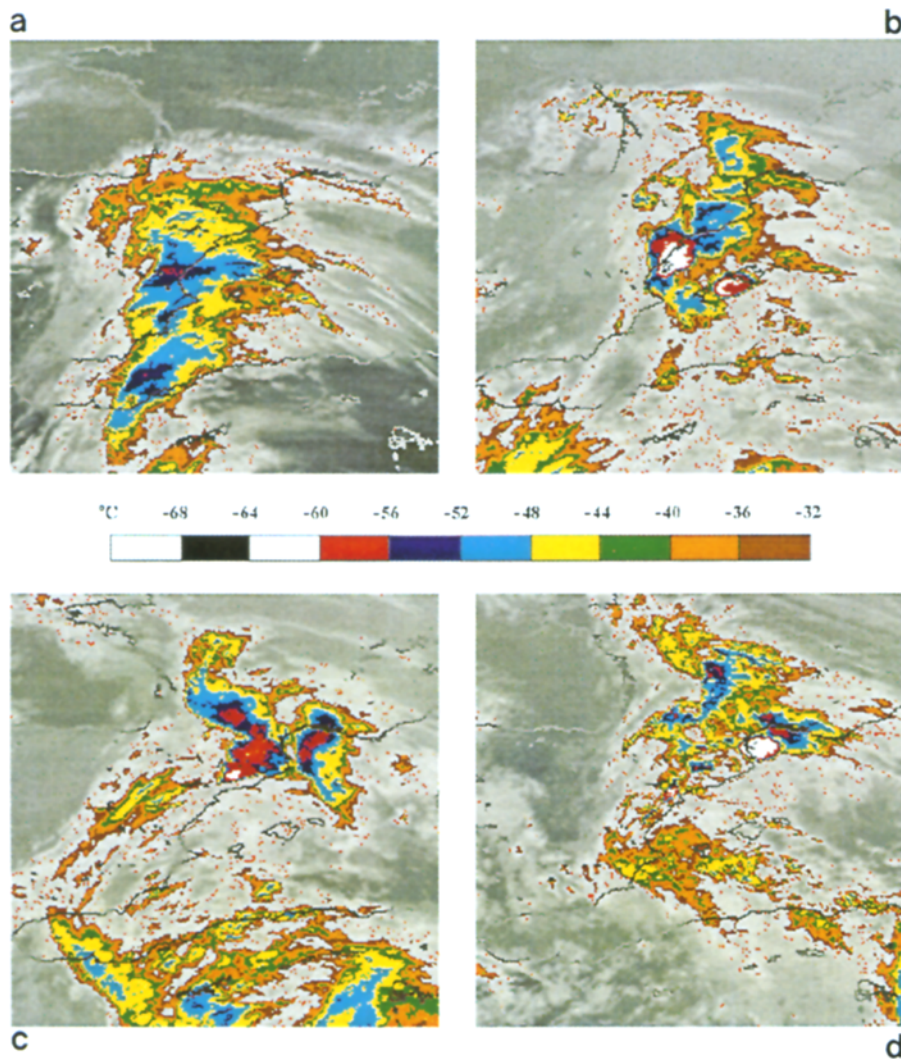


Fig. 4. Infrared Meteosat image for (a) 12 UTC 9 October 1994, (b) 21 UTC 9 October 1994, (c) 06 UTC 10 October 1994, (d) 15 UTC 10 October 1994

east from its situation 18 hours before. Warm air remains over the western Mediterranean at all levels of the troposphere.

Meteosat image at 12 UTC 9 October, (Fig. 4a), shows a band of clouds over the eastern coast of Spain with embedded convection over and south of the Valencia region. During the evening, convection became deeper as shown by Fig. 4b, and moved slowly towards the northeast, reaching Catalonia during the night. Deep and stationary convection affected south Catalonia early in the morning of 10 October during several hours (Fig. 4c), and after it moved northwards (Fig. 4d).

From the synoptic charts and satellite images, it can be seen that deep convection did not develop close to the trough of middle and upper levels, where vorticity advection is appreciable, but in between the trough and the ridge axes close to the ridge, where no appreciable vorticity centres can be easily identified on ECMWF charts. A similar scenario was observed previously for another convective heavy rain event in Catalonia in October 1987 (Ramis et al., 1994).

3. Diagnostic Study

Forecasting and/or diagnosing deep convection producing heavy rain includes an evaluation of different ingredients and their possible contribution and interactions. These ingredients go from synoptic scale, which has to produce the favourable environment, to mesoscale, which provides the lifting mechanisms for low-level parcels (Doswell, 1987). Ingredients from synoptic scale can be evaluated from gridded numerical analysis or forecasts at that scale. Upward vertical motion, water vapour convergence at low levels, high water vapour content in a deep atmospheric column, and potential or latent instability, have been identified as favourable mechanisms (Maddox et al., 1979). Quasi-geostrophic theory can be used to determine vertical motion (Hoskins and Pedder, 1980). Water vapour convergence can be calculated from the flux of specific humidity. Water vapour content can be represented by the precipitable water (PW). Potential instability for the low troposphere can be determined by means of the difference of equivalent potential temperature between two levels (e.g., 500 and

1000 hPa), and latent instability can be determined by means of the CAPE. A more detailed study on the vertical stability of the air masses to complement the gridded data analysis can be obtained through the analysis of radiosounding data.

Mesoscale mechanisms are much more complex. They can go from physical effects (orographically induced convection), kinematic effects (convergence lines), mixed orographic-kinematic effects (Ramis et al., 1994), or dynamic effects [ageostrophic motion associated with short wave troughs or jet streaks at upper levels (Rockwood and Maddox, 1988), interaction between two upper jet streaks (Hakim and Uccellini, 1992), gravity waves (Uccellini, 1975), conditional symmetric instability (Emanuel, 1983) or coupling of upper and lower jet streaks (Uccellini and Johnson, 1979)].

In this sense, deep convection can be considered as a typical example of interaction between scales. Large scale provides the appropriate environment, and mesoscale mechanisms determine when and where convection will develop.

3.1 Synoptic Diagnosis

Diagnosis products have been calculated using gridded analysis from the ECMWF (0.75 degrees of latitude/longitude resolution). Large scale upward forcing for vertical motion, calculated from the divergence of the Q vector (Hoskins and Pedder, 1980), is shown in Fig. 5a for 12 UTC 9 October. At low levels an upward maximum centre related with the strong warm advection is located over southeastern Spain, and less values are found over northeastern Spain. At medium levels, the upward forcing is weak and it is found in the areas where there is positive vorticity advection.

The location of the temperature advection in the low troposphere is represented by the helicity (Davies-Jones et al., 1990) between 1000 and 700 hPa (Fig. 5b), since the helicity can be considered as a measurement of the integrated temperature advection between the considered levels (Tudurí and Ramis, 1997). It can be observed that the zone with maximum values of helicity corresponds to the area with the strongest upward forcing at low levels (Fig. 6a).

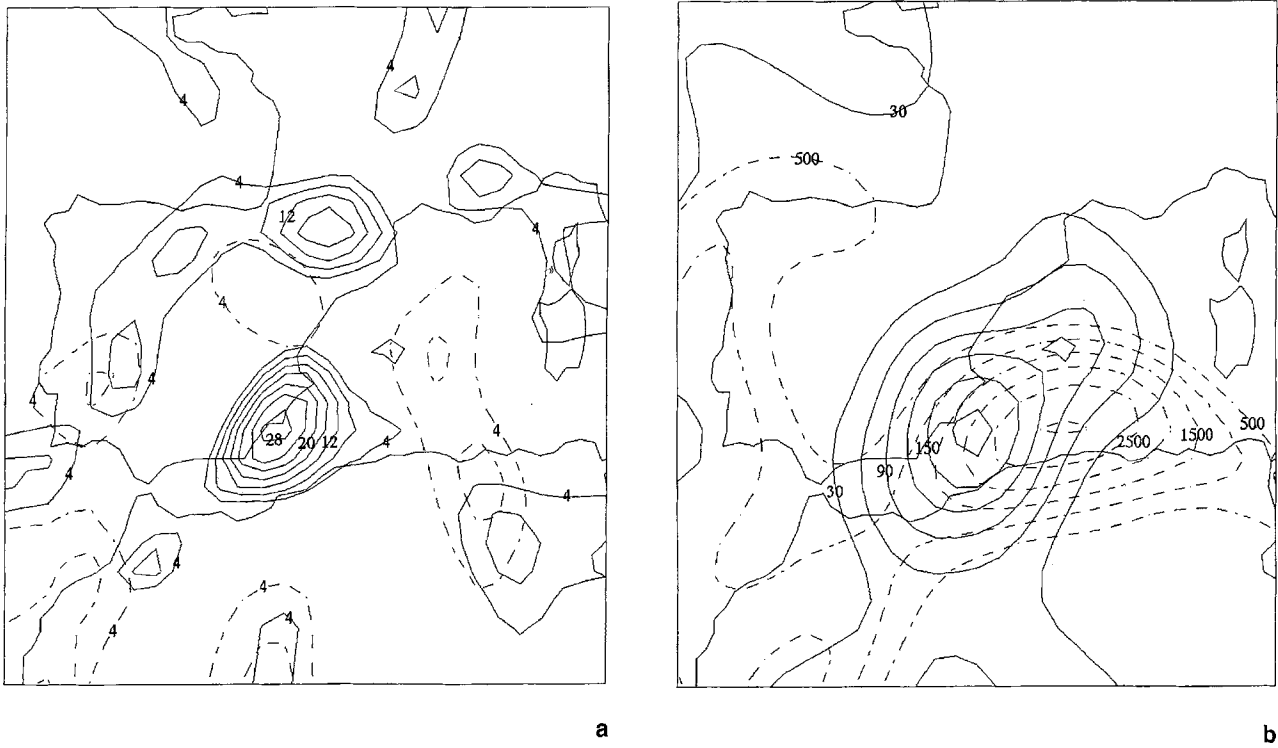


Fig. 5. For 12 UTC 9 October 1994: (a) Upward quasigeostrophic forcing at 925 hPa (continuous line) and at 500 hPa (dashed line) (contour interval is $4.10^{-18} \text{ m kg}^{-1} \text{ s}^{-1}$ starting at $4.10^{-18} \text{ m kg}^{-1} \text{ s}^{-1}$); (b) Positive helicity (continuous line; contour interval is $30 \text{ m}^2 \text{ s}^{-2}$ starting at $30 \text{ m}^2 \text{ s}^{-2}$) and CAPE (dashed line; contour interval is 500 J kg^{-1} starting at 500 J kg^{-1})

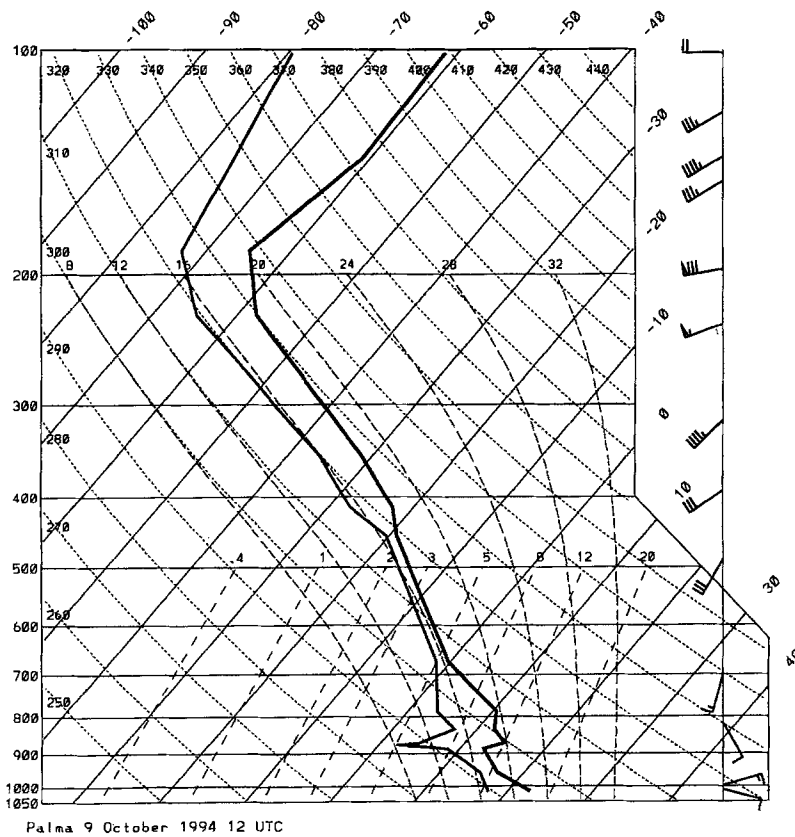


Fig. 6. Radiosounding on 12 UTC 9 October 1994 at Palma (Pa in Fig. 1)

Spatial distribution of CAPE (Fig. 5b) shows that the greatest values appear over the south of the western Mediterranean. Analyses of the radiosonde data at this time from Palma, Murcia and Zaragoza (see Fig. 1 for locations) show that ECMWF analyses give a good representation of the actual latent instability of the environment in the area of interest. In fact, over Palma, (Fig. 6), although a LID (Farrel and Carlson, 1989) structure is present, CAPE is 850 J kg^{-1} and the energy that inhibits convection is 36 J kg^{-1} . In addition, the Lifted index (LI) is -1 , the K index (KI) 31, and the Total Total's index (TT) 48. The humidity is very high in all the troposphere leading to a PW of 40 mm. Winds are from the east at low levels, veering to the southwest at 700 hPa (helicity is $83 \text{ m}^2 \text{ s}^{-2}$), but no evidence of LLJ exists at that time. Although the launched balloon over Murcia only attained 700 hPa, the available data show strong southerly winds in the layer 800–700 hPa, suggesting the existence of a LLJ. The wind also veers from the east to the south indicating the presence of warm advection. Over Zaragoza, the atmosphere is quite stable as a consequence of a strong inversion close to the ground. Stability indices do not exhibit high probability of convection since $\text{LI}=6$ and $\text{TT}=45$. The PW is 30 mm. The wind is weak at low levels but also indicates warm advection with an helicity of $50 \text{ m}^2 \text{ s}^{-2}$.

A composite chart showing where quasi-geostrophic upward forcing at 850 hPa, water vapour convergence in the layer 1000–850 hPa and convective instability between 1000 and 500 hPa overlap, is shown in Fig. 7. Southeast Spain is then an area where the favorable mechanisms for convective developments are all present.

Another diagnosis for vertical motion can be deduced from the wind fields by looking for convergence zones at low levels and taking in mind the continuity equation. Figure 8 shows the ageostrophic irrotational wind field, obtained using the Endlich (1967) method, and relative humidity, both at 925 hPa. It can be seen that there is convergence over eastern Spain precisely where relative humidity is very high. The ageostrophic wind is probably associated with the isallobaric wind generated as a consequence of a deep pressure fall ($2.5 \text{ hPa}/3 \text{ h}$) observed in the Murcia coast.

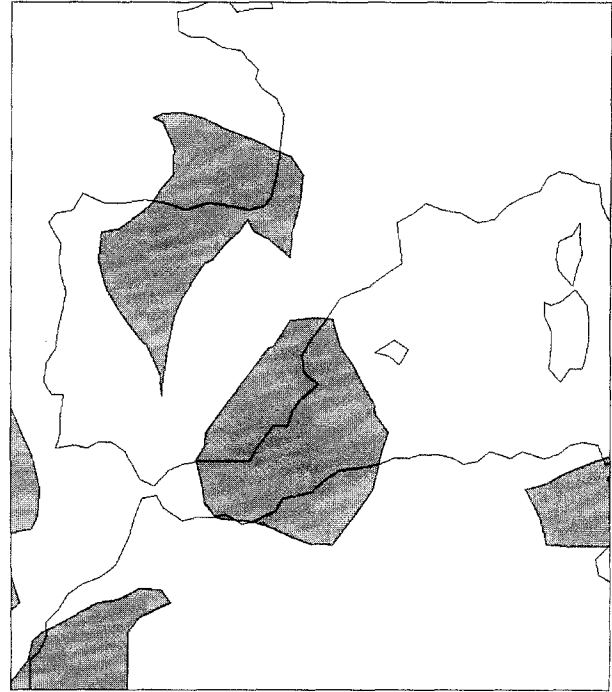


Fig. 7. Composite chart for 12 UTC 9 October 1994. The shaded zones denote the existence of upward quasigeostrophic forcing at 850 hPa, potential instability between 500 and 1000 hPa and moisture convergence in the 1000–850 hPa layer

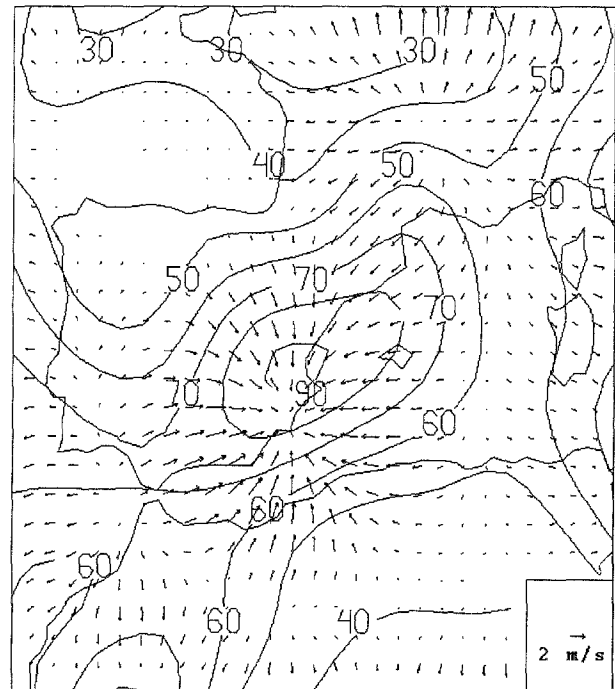


Fig. 8. Irrotational component of the ageostrophic wind and relative humidity (in %) at 925 hPa on 12 UTC 9 October 1994



Fig. 9. Upslope flow on 12 UTC 9 October 1994. Contour interval is 1 cm s^{-1} starting at 1 cm s^{-1} (continuous line) and at -1 cm s^{-1} (dashed line)

Orographic forcing can be quantified by means of the upslope component, calculated using the orography h and the surface wind \vec{V} as

$$w = \vec{V} \cdot \nabla h \quad (1)$$

Figure 9 shows this orographic forcing at the ECMWF data resolution. Upslope motion exists along the Spanish Mediterranean coast, and hence the orography also represents a lifting mechanism for the parcels reaching the coast from the sea.

In summary, on 12 UTC 9 October, the necessary ingredients for deep convection, deduced from dynamical mechanisms (Fig. 7), seem to be present over eastern and southeastern Spain and south of the western Mediterranean. In addition, these ingredients are supplemented by important orographic forcing and convergence of moist air over eastern Spain. Therefore, the diagnosis at synoptic scale suggests that the deepest convection is more likely in that area. This is consistent with Meteosat image at 12 UTC 9 October, (Fig. 4a).



Fig. 10. Composite chart for 06 UTC 10 October 1994. The shaded zones denote the existence of upward quasigeostrophic forcing at 850 hPa, potential instability between 500 and 1000 hPa and moisture convergence in the 1000–850 hPa layer

Similar diagnostic products have been obtained for successive (6 hours interval) during the episode. The changes observed in the spatial distribution of the dynamic and thermodynamic mechanisms indicate a displacement of the zone favourable for convection towards the north following the Spanish Mediterranean coast (see Figs. 10 and 11). In addition, the strongest orographic forcing signal is moved over Catalonia.

Radiosonde data from Palma at 00 UTC 10 October is not available. At 12 UTC, (Fig. 12), the LID structure is clear although the inversion is weak. This sounding yields a CAPE of 2900 J kg^{-1} , an inhibition energy of 6 J kg^{-1} , a LI of -4 , a TT of 44, and very high humidity in all the troposphere resulting in 41 mm of PW. A clear southerly LLJ can be identified at 700 hPa. Over Murcia at 00 UTC 10 October (sounding not shown) the CAPE is 470 J kg^{-1} , the inhibition energy 90 J kg^{-1} , the LI is -1 , the TT is 45 and the PW 37 mm. The atmosphere is very humid at low levels but there is a dry layer

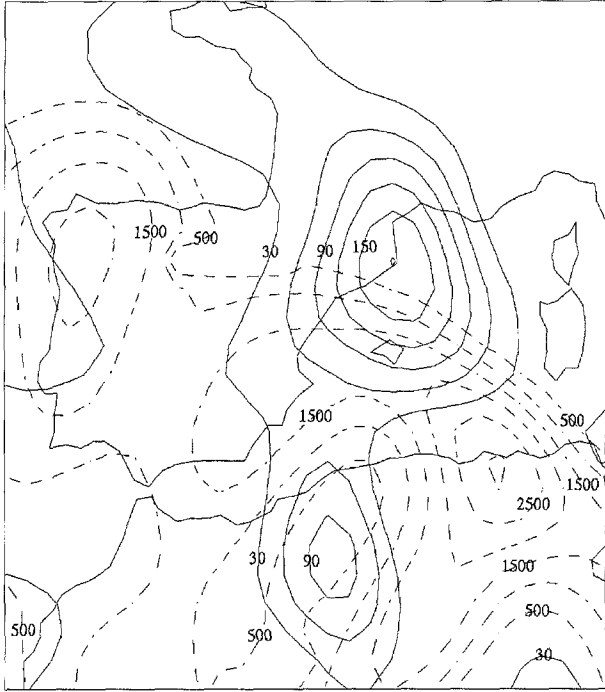


Fig. 11. Positive helicity (continuous line; contour interval is $30 \text{ m}^2 \text{ s}^{-2}$ starting at $30 \text{ m}^2 \text{ s}^{-2}$) and CAPE (dashed line; contour interval is 500 J kg^{-1} starting at 500 J kg^{-1}), on 06 UTC 10 October 1994

between 600 and 300 hPa. No evidence of LLJ appears at that time, although warm advection continues since helicity is $40 \text{ m}^2 \text{ s}^{-2}$. Over Zaragoza at the same time (sounding not shown) the atmosphere is very stable (CAPE = 0), with a strong inversion at low levels.

In summary, on 10 October between 00 and 12 UTC, in which time interval the heaviest precipitation occurred in Catalonia, the synoptic ingredients for heavy rain have reached Catalonia, where orographic forcing is also maximized. The analysis of the radiosonde data from Palma, Murcia and Zaragoza reveals that the air mass over the Balearic Islands is the most representative of the environment in which convection developed. The wind at low levels is advecting this air mass towards Catalonia, where the important orographic forcing would facilitate the breaking of the LID and the release of the instability. The high stability over Zaragoza indicates the presence of a sharp boundary between the Mediterranean air mass supporting the convection, and that over inland Spain (see Fig. 4b, c).

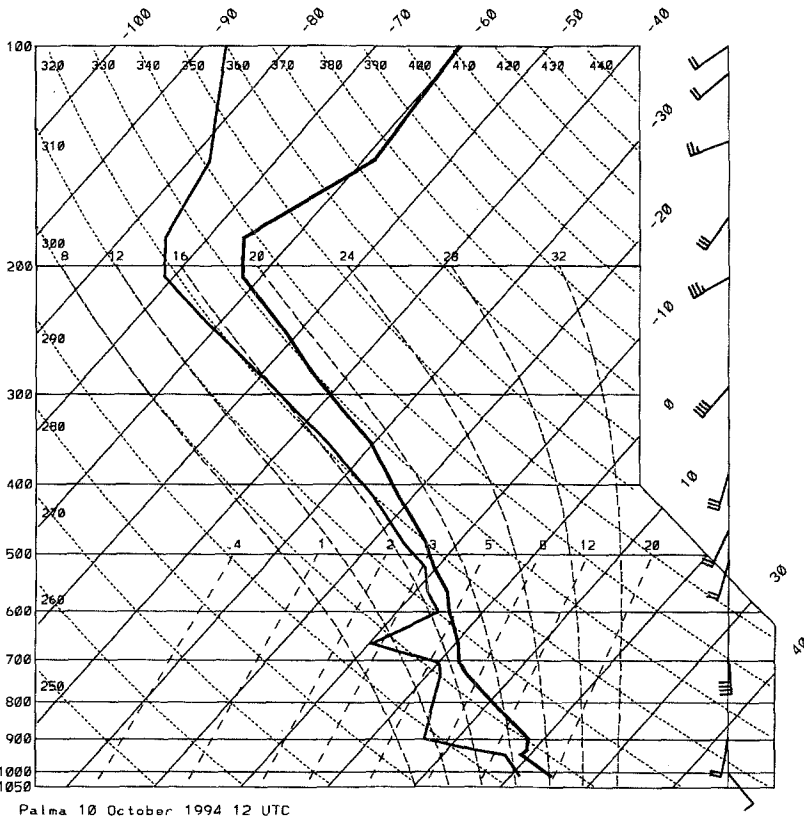


Fig. 12. Radiosounding on 12 UTC 10 October 1994 at Palma (Pa in Fig. 1)

3.2 Air Masses Back Trajectories

Back trajectories provide information about the path of the air masses. If these trajectories are calculated on isentropic surface, the method provides also information about the vertical motion of the air parcels.

By interpolation of data from the available isobaric surfaces, values of geopotential, temperature and wind components on several isentropic surfaces have been obtained following the methodology described in Duquet (1964). Position and velocity of the parcel are calculated by using the kinematic formulas with a time step of 900 seconds. A full description of the method can be found in Alarcón (1993).

Figure 13 shows the 3 days back trajectories of several parcels located over the Spanish Mediterranean coast on the 310 K isentropic surface. It can be seen that the parcels come from the south. Its vertical position shows that there is a general upward motion over the Spanish coast which is in agreement with the previous diagnosis. The back trajectories on the 295 K surface (not shown) indicate that the air parcels mainly come from the east, with a long path over the sea. That history of the air mass is in agreement with the findings of Tudurí and Ramis (1997), which show that most of the torrential rainfalls in the Balearic Islands are produced with warm air in all the troposphere.

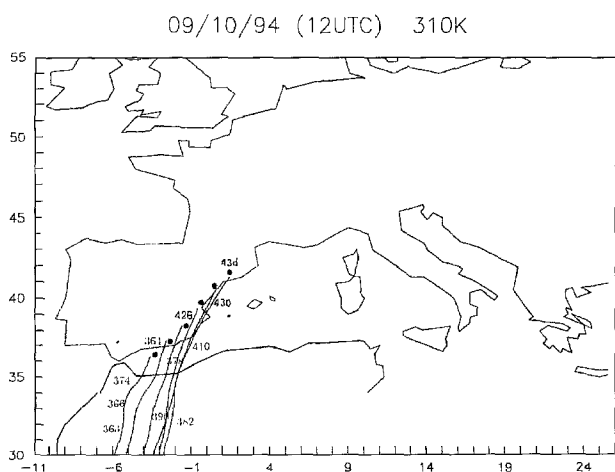
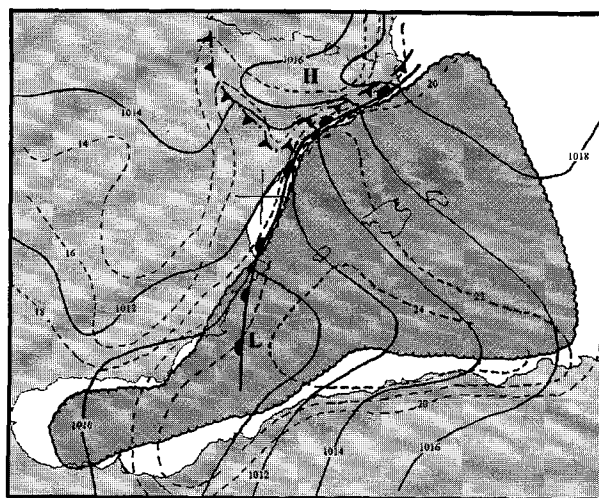


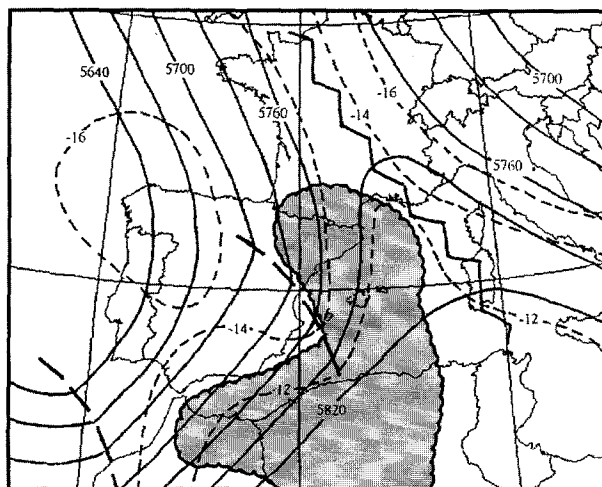
Fig. 13. 3-days back trajectories of some parcels located over eastern Spain on the 310 K isentropic surface starting on 12 UTC 9 October 1994. Labels indicate height in dam

3.3 Subsynchronous Study

Surface subsynoptic analyses have been constructed by using all the available information over the area of interest. When doing the analyses, we have taken into account the effects induced by the Atlas and the Pyrenees on the pressure field. That is, since the flux at medium and upper levels blows almost perpendicular to these mountain ranges, a pressure dipole structure (cyclone in the lee and anticyclone in the



a



b

Fig. 14. (a) Subjective surface mesoscale analysis for 06 UTC 10 October 1994; continuous lines represent isobars, dashed lines isotherms and the dark shaded area represents the zone with dew point higher than 18°C. (b) Subjective 500 hPa surface reanalysis on 00 UTC 10 October 1994; continuous lines represent height, dashed lines isotherms and the dark shaded area represents the zone with relative humidity greater than 80%

windward) develops (Bessemoulin et al., 1993). In addition, Meteosat images and conceptual models of pressure distribution around a thunderstorm (Schofield and Purdom, 1986) have been considered. This is useful to mitigate the problem of the sparsity of the data.

The analysis show that at the beginning of the event the low in the lee of the Atlas produces a strong and humid flux toward the Murcia and Valencia regions. Progressively, as the low moves northwards, the strongest flux focuses towards Catalonia (Fig. 14a). At the same time the humid air also displaces northwards. Figure 14b shows a reanalysis of the 500 hPa surface on 00 UTC 10 October. Available data and the Meteosat image at that time suggest the presence of a secondary trough over northeastern Spain. In the ECMWF analyses, this trough is weaker and located downstream over southwest France.

Considering these analysis and the satellite pictures, it is deduced that the most important convection developed by interaction of the humid flux against the coastal mountains, and ahead of the secondary trough at upper levels. Although orographic forcing is general over coastal Spain (Fig. 9), convection only progresses northwards as the humid air does, in connection with the displacement of the surface low. However, the convection was almost stationary during several hours over south Catalonia where the centres of maximum precipitation occurred. This fact can be related to the convergence between the easterly general flow and the outflow from the high pressure developed in the windward of the Pyrenees. The high pressure limits define a true cold front as it is revealed by the isotherms (Fig. 14a).

The previous scenario matches in many aspects the situation described by Maddox et al. (1979) as a “mesohigh event” for flash floods in USA. In fact, the event occurred near the ridge axis and far from the large scale trough that appears on the 500 hPa analysis. Warm and humid surface air is advected towards the mesohigh and convergence exists in the boundary of this mesohigh. At 850 hPa the LLJ also feeds the convection with moist air. At medium levels, a secondary trough favours the vertical motion over the area with convergence at low levels. And the humidity is very high in all the troposphere, so favouring the precipitation efficiency.

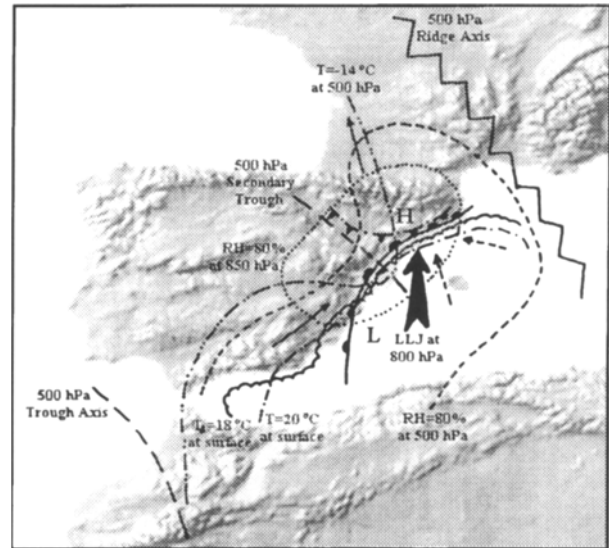


Fig. 15. Scheme representing the scenario at 06 UTC 10 October 1994. H and L represent the position of the mesohigh and the mesolow at surface. Dashed arrows represent the flux at surface and continuous arrows the flux at 500 hPa

The major difference between our scenario and that described by Maddox et al. (1979) is that the mesohigh is not produced by previous thunderstorms, but by the Pyrenees, which creates an anti-cyclone in the windward side relative to the large scale flux at medium and high levels. Temperature and humidity at surface demonstrate that there is a true cold front around the mesohigh, which plays the same role that the front produced by thunderstorm downdrafts. In addition, the low producing the warm and humid advection towards Catalonia is, at least during the first stage, a consequence of the orographic action of the Atlas mountains on the synoptic flux. Finally, a particular aspect in our case is that the orographic lifting forced by the coastal mountains of Catalonia enhances the lifting produced by the convergence along the mesohigh boundary, and helps to trigger and maintain the convection. A scheme of this scenario is presented in Fig. 15.

4. Numerical Simulations

The simulations presented were performed using the hydrostatic meso- β numerical model developed by Nickerson et al. (1986). The characteristics of the used version can be found in Romero et al. (1997), with the exception that for the

Table 1. Summary of the Numerical Experiments Performed for 9 and 10 October 1994 in Order to Isolate the Effect of the Orography and Evaporation from the Sea. Note that except for the Orography and Latent Heat Flux at the Sea Surface, the Rest of Parameters are Initially the same for the four Simulations

Experiment	Orography	Sea evaporation
f_0	NO	NO
f_1	YES	NO
f_2	NO	YES
f_{12}	YES	YES

present experiments the cumulus convection parameterization scheme of Kain and Fritsch (1990) has been used.

A set of simulations has been carried out for 9 and 10 October 1994, in order to test the capability of the model to forecast the event, and to assist the assessment of the main physical processes that controlled the occurrence of the coastal heavy precipitation. Table 1 summarizes the four experiments performed for each day. Implicitly, we are considering the coastal topography and the latent heat flux from the warm Mediterranean sea as key factors responsible for the focalization of the heavy rainfall in the coastal areas of eastern Spain.

Following the reasoning of Stein and Alpert (1993), the outputs (e.g., rainfall) of the four experiments listed in Table 1 may be algebraically combined to yield the isolated effects on the considered field by the orography, evaporation from the sea, and their synergism:

1. Effect of the orography $f_1^* = f_1 - f_0$
2. Effect of the sea evaporation $f_2^* = f_2 - f_0$
3. Effect of the interaction orography - sea evaporation $f_{12}^* = f_{12} - (f_1 + f_2) + f_0$

ECMWF analysis on standard pressure levels, at 00, 06, 12 and 18 UTC, have been used to initialize the model and to supply the time-dependent boundary conditions. Initial imbalances of the interpolated fields are reduced by minimizing the vertical integral of the horizontal divergence (Pinty, 1984). It should be noted that the initial fields in experiments f_0 and f_2 (without orography; Table 1) could be not absolutely free of orographic influence, since they are based on forecasts and observations which in turn contain orographic effects.

The model orography is linearly interpolated at grid points from the NGDC/NOAA data base

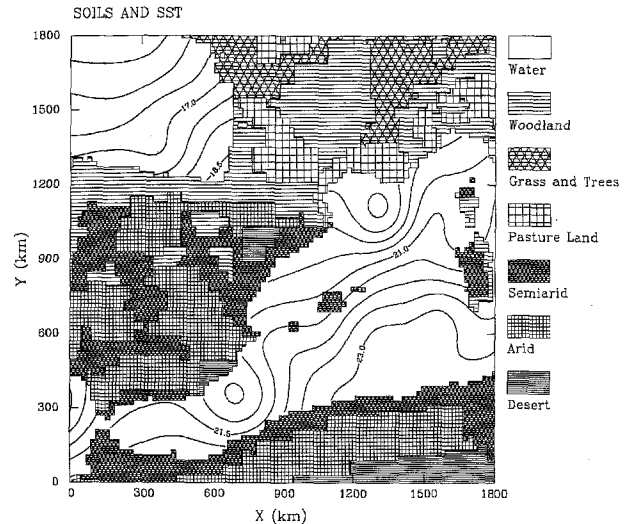


Fig. 16. Distribution of surface types in the model domain and sea surface temperature ($^{\circ}\text{C}$) for the numerical simulations

(5 minutes resolution) and smoothed by a two step filter (Shapiro, 1970). Using NOAA-AVHRR mosaics and atlas information, a spatial distribution of seven land types was derived for the western Mediterranean region. Subsoil temperature corresponds to the October climatological value, and sea surface temperature (kept constant during the simulation) is provided by the ECMWF surface data. Figure 16 shows the sea surface temperature and soil types considered in the simulations.

The model domain (Fig. 16) is centered at (1°E , 41°N) under a polar-stereographic map projection and covers $1800 \times 1800 \text{ km}^2$ (91×91 grid points with an horizontal grid length of 20 km). In the vertical, 30 levels have been considered, the first one being approximately 4.5 m above the ground. For each day, the simulations extend 30 h , from 00 UTC till 06 UTC (next day), since we intend to compare the forecast rainfall for the last 24 h (free of model spinup influences), with the observed rainfall for 07–07 UTC (Fig. 2).

4.1. Results for 9 October

Forecast fields at 18 UTC show that at low levels (Fig. 17) a very well marked trough is located over the Algerian coast in the lee of the Atlas range. It is also remarkable the strong warm anomaly over the same area. Both aspects combine to produce warm advection over the

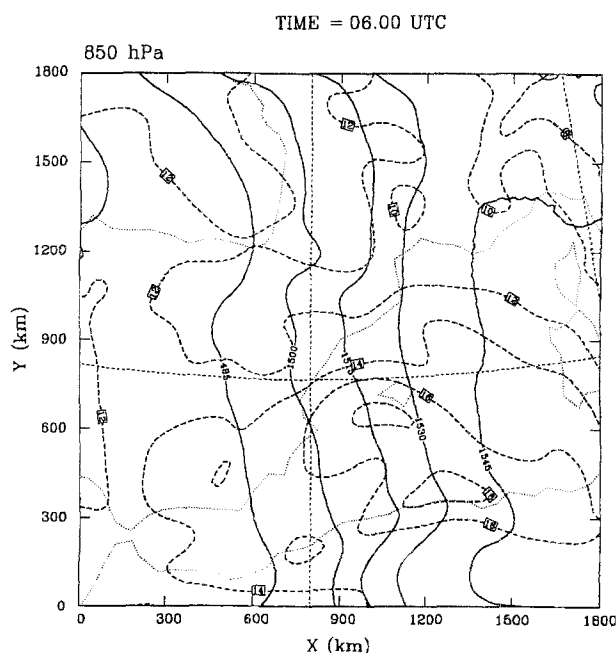
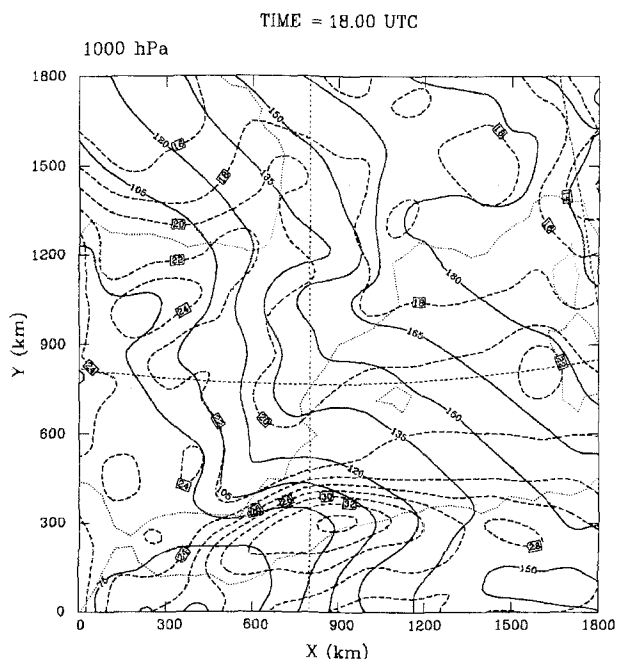
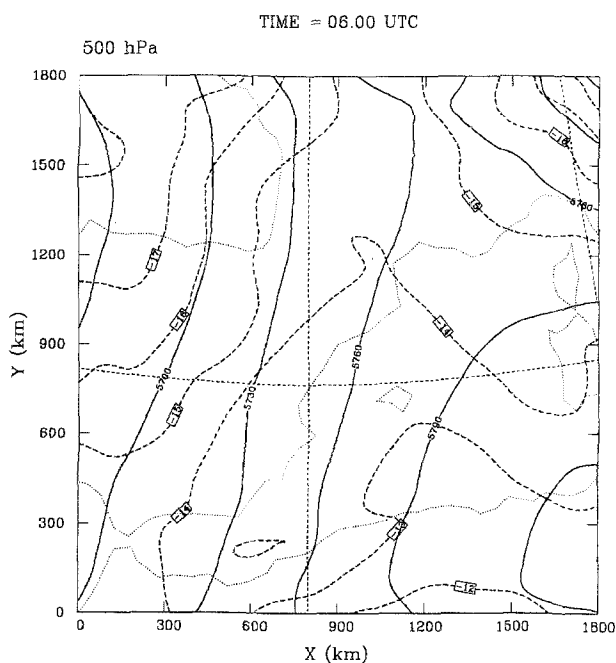
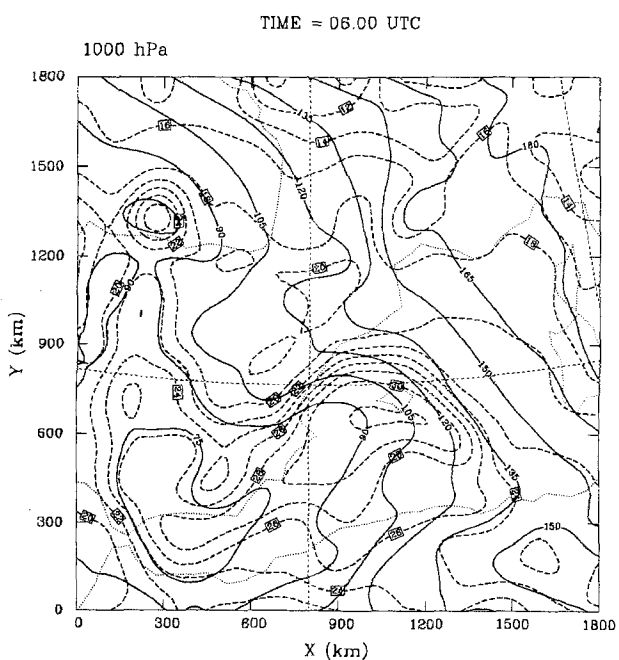


Fig. 17. Forecast fields on 18 UTC 9 October 1994 at 1000 hPa, showing height (gpm, continuous line) and temperature ($^{\circ}\text{C}$, dashed line)

south of the Valencia region. An anticyclonic circulation is present over northeastern Spain as a feature of the pressure dipole across the Pyrenees. Such pressure distribution produces an easterly flux over the Mediterranean, impinging almost perpendicular on the Spanish coast, notably over Valencia. At 850 hPa (not shown)



a

c

Fig. 18. Forecast fields on 06 UTC 10 October 1994, showing height (gpm, continuous line) and temperature ($^{\circ}\text{C}$, dashed line): (a) 1000 hPa, (b) 850 hPa, (c) 500 hPa

the flux is from the south, with the strongest winds, 15 ms^{-1} , over southeastern Spain, where well marked warm advection is identified. At upper levels, the flux is from the south-southwest over the Mediterranean and eastern Spain, where warm advection also occurs.

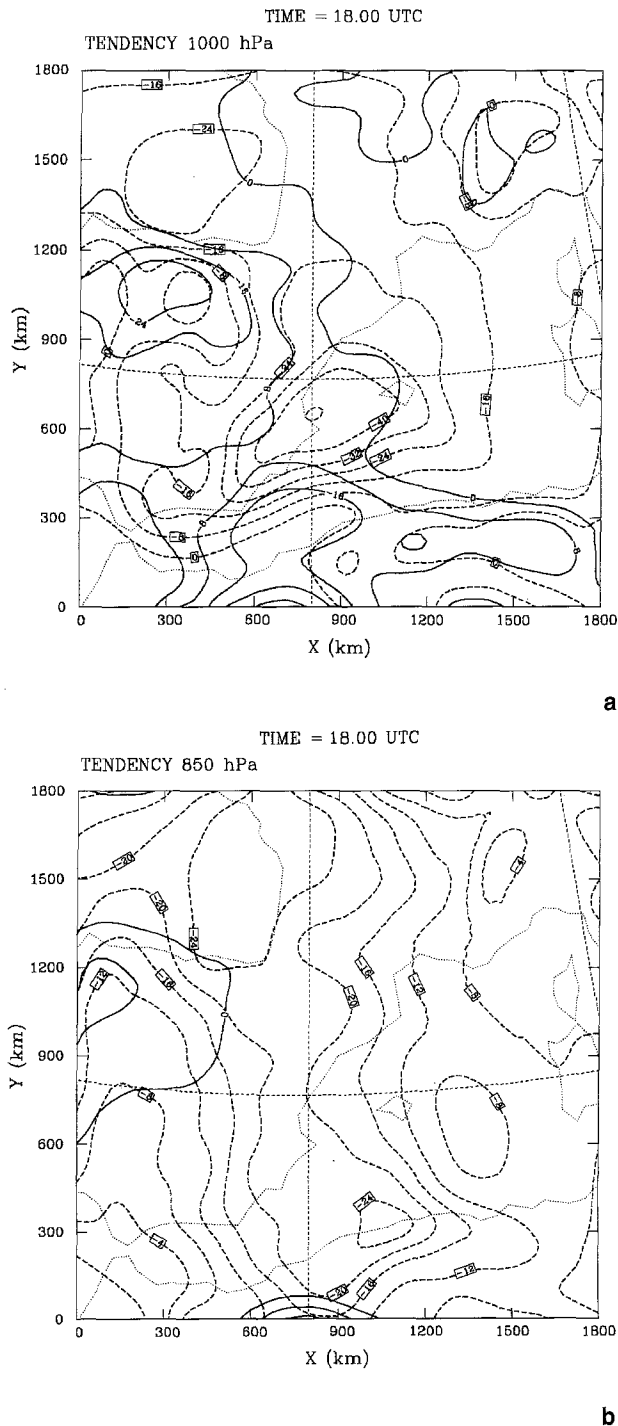


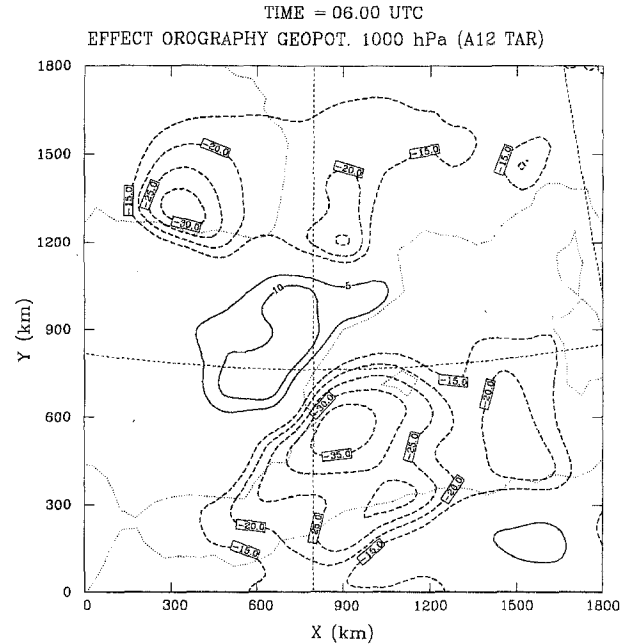
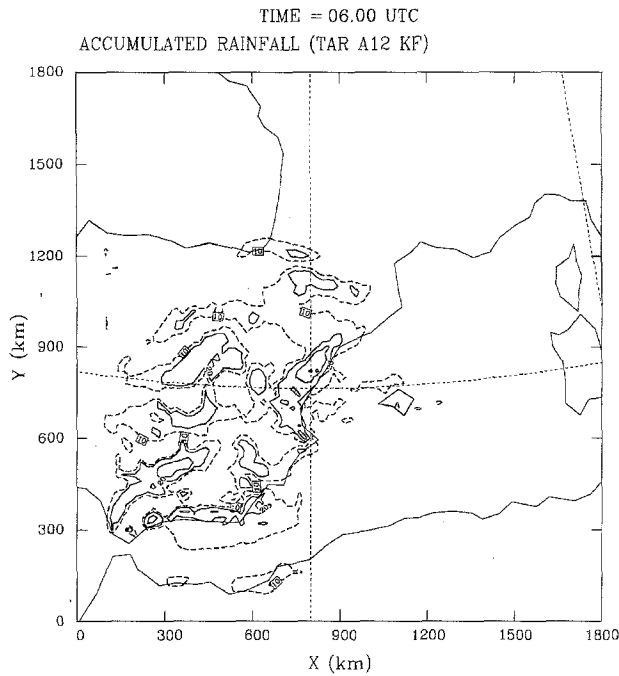
Fig. 19. Model predicted geopotential negative tendency between 06 UTC and 18 UTC 9 October 1994 (continuous line) and between 18 UTC 9 October 1994 and 06 UTC 10 October 1994 (dashed line): (a) at 1000 hPa, (b) at 850 hPa

Forecast fields at 06 UTC 10 October show that at 1000 hPa (Fig. 18a) the low has moved to the north along the Mediterranean coast. A strong geopotential gradient appears to the northeast of the low (over the Balearic Islands), producing an easterly flow towards north Valen-

cia and south Catalonia. The pressure dipole in the Pyrenees continues in spite of the general pressure decrease in the domain. The warm anomaly has moved also to the north, producing a very well marked thermal boundary along the Valencia-Catalonia coast. At 850 hPa (Fig. 18b), the southerly flux exhibits a band of maximum winds from the Algerian coast to Catalonia. As a consequence of these winds, there is notable warm advection towards Catalonia. At 500 hPa (Fig. 18c) the flux continues from the south-southwest over the Mediterranean and eastern Spain, but stronger cyclonic circulation appears at the west of the domain. A thermal ridge is depicted over the western Mediterranean.

As an illustration of the pressure changes at surface, Fig. 19a shows negative values of geopotential tendency at 1000 hPa given by the model between 06 UTC and 18 UTC 9 October, and between 18 UTC 9 October and 06 UTC 10 October. In the first case, the maximum values are located along the Algerian coast, so inducing a strong increase of the geopotential gradient to the southeast of Spain. This explains why the wind increased strongly in this area, and consequently the warm advection towards Spain. In the second time interval the greatest negative tendency occurs close to the Valencia coast. This structures implies an intensification of the geopotential gradient over the Balearic Islands, so enhancing the onshore flow towards Catalonia. Also interesting is the tendency field at 850 hPa (Fig. 19b). The most significant feature is found between 18 UTC 9 October and 06 UTC 10 October. A large increase of the geopotential gradient is forced between Algeria and Catalonia, so favouring the strengthening of the LLJ.

Forecast rainfall for this day is shown in Fig. 20. In general terms, it compares favourably with the observed precipitation over eastern Spain (Fig. 2a). However, as usually occurs in meso- β scale simulations of convective events, the model clearly underestimates the records (only in northern Valencia 60 mm are slightly exceeded). In addition, the model gives an unobserved pattern over the Mediterranean coastal fringe of Andalucía, and underestimates and locates slightly southwards the most important maximum present in the southern extreme of Catalonia. If only the convective contribution is considered (figure not shown), it is concluded



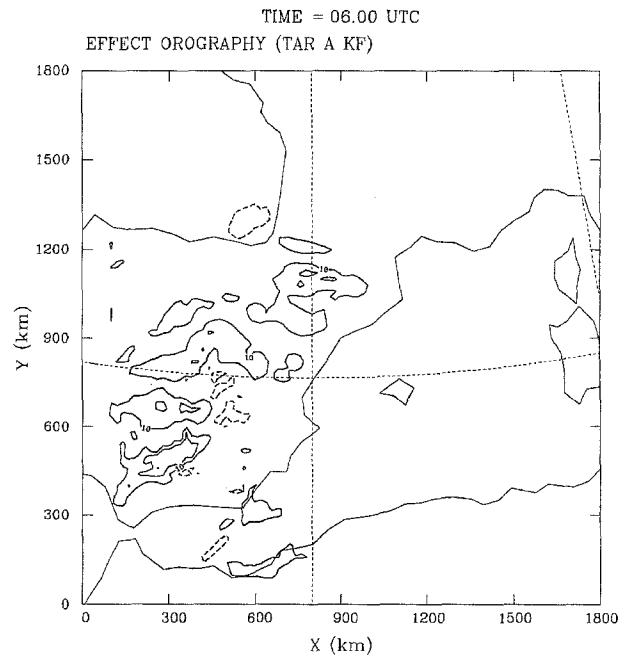
a

Fig. 20. Forecast total precipitation from 06 UTC 9 October 1994 to 06 UTC 10 October 1994. Contour interval is 20 mm starting at 20 mm (continuous line). Dashed contour represents 10 mm

that, except in the area of the Pyrenees, the forecast rainfall is essentially convective.

If simply the basic experiment is considered (f_0 in Table 1), then the forecast rainfall is quite deficient. Significant rainfall is only obtained in inland areas, and less than 10 mm are given by the model over all the eastern coast of Spain. This result clearly confirms that only dynamic forcing is not sufficient to focalize the coastal rainfall maxima observed in these convective events. Rather, the synoptic scale is only responsible for the creation of the appropriate conditions for convection development.

The effect of the orography on the 1000 hPa geopotential field at 06 UTC 10 October is shown in Fig. 21a. This picture confirms that the trough developed over the Mediterranean, in the lee of the Atlas, has a topographic cause. Similarly the pressure dipole produced by the Pyrenees is clearly isolated. It is notable that the windward positive tendency extends its influence toward central Spain. In general terms, the orographic effect on the low-level wind (not shown) exhibits a cyclonic circulation over the western Mediterranean, in agreement with the geopotential anomalies produced by the orography. The orographic action on the 1000 hPa



b

Fig. 21. Effect of the orography at the end of the simulation (06 UTC 10 October 1994): (a) on the geopotential field at 1000 hPa (in gpm); (b) on the total precipitation (contour interval is 20 mm starting at 10 mm, continuous line, and at -10 mm, dashed line)

temperature (not shown), represents a warming effect over south Mediterranean and a cooling effect over northeastern Spain. The combination of both effects explains the accentuated temperature gradient over eastern Spain and between

Catalonia and the Balearic Islands (Fig. 18a). For the rainfall, the effect is important, but mainly limited to the interior relief systems (Fig. 21b). This is in agreement with the model initial conditions for relative humidity at low levels (not shown) which indicates high values of relative humidity over eastern Spain but not over the Mediterranean.

The effect of the evaporation from the sea on geopotential, wind and temperature at surface is negligible. On the accumulated rainfall it is weak and, as expected, mainly positive. In this case it affects coastal areas of Catalonia, Valencia and eastern Andalucía. It seems that, without presence of orography, the evaporation from the sea does not contribute decisively to the rainfall field.

The most decisive role to define the coastal rainfall maximum in the Valencia area was exerted by the synergistic factor (see Fig. 22). Other positive signals exist over the sea and coastal zones, and the action is suppressive in many interior areas. Therefore, it seems that in its initial state, the low atmosphere over the sea did not have enough moisture content to readily feed the coastal convection. Evaporation heat fluxes during the course of the simulation from the Mediterranean are very high to the south and southwest of the Balearic Islands (exceeding

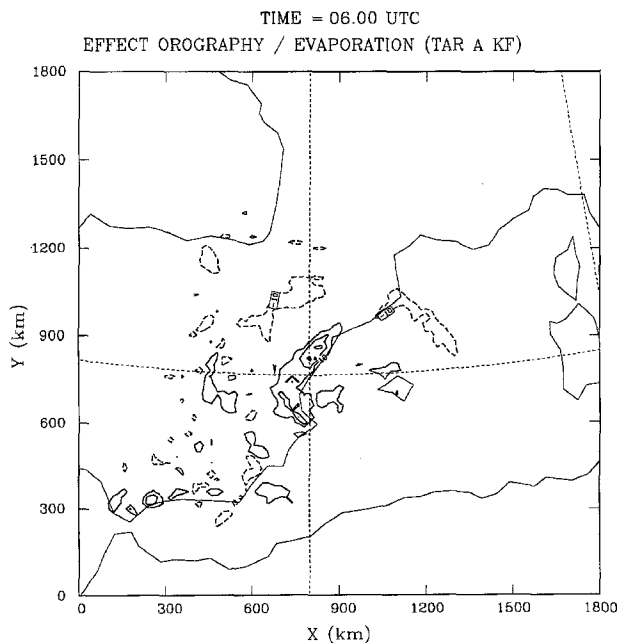


Fig. 22. Effect of the interaction orography/evaporation at the end of the simulation (06 UTC 10 October 1994) on the total precipitation (contour interval is 20 mm starting at 10 mm, continuous line, and at -10 mm, dashed line)

300 W m^{-2}), charging of moisture the air parcels that interact downstream with the coastal topography. The effect of the interactive factor on the wind field (not shown) is also weak in this case. It is most notable over Valencia and south Catalonia where it acts producing a slight upslope component (opposite to the orographic action), probably because moist flows present smaller effective stability and therefore are less susceptible to blocking. The effect on the 1000 hPa geopotential is weak and only slightly significant over south Valencia where a negative signal appears, in agreement with the effect on the surface wind field.

4.2 Results for 10 October

Figure 23 shows the 18 hours forecast fields at 18 UTC 10 October. At low levels (Fig. 23a), it is seen that the low located over south Spain (see Fig. 18a) has displaced to the east and has weakened. However, the strong flux from the southeast over the Mediterranean remains practically over the same that 12 hours before, blowing towards the northern part of the Catalonia coast. The warm tongue over the western Mediterranean, although less intense, maintains its structure and then warm advection continues over Catalonia. The orographic pressure dipole about the Pyrenees is still present. At 850 hPa (not shown) the geopotential gradient over the Mediterranean has weakened but the flux remains from the south with the strongest values located over north Catalonia and south France. At upper levels (Fig. 23b) the flux keeps its south-southwest component but it is much weaker than 12 hours before (Fig. 18c). This fact can explain why the orographic effects on the surface pressure field in the lee of the Atlas are smoother than the day before, as it will be shown later.

As commented previously, on this day the heavy rains affected northern Valencia and south Catalonia as on 9 October, but in contrast, the coastal part of northern Catalonia was also extensively affected by convection whereas southeastern Spain was free of important rains (see Fig. 2b). This spatial rainfall distribution is well captured by the mesoscale model, as can be seen in Fig. 24. A coastal band of more than 40 mm, resembling the observed pattern, is

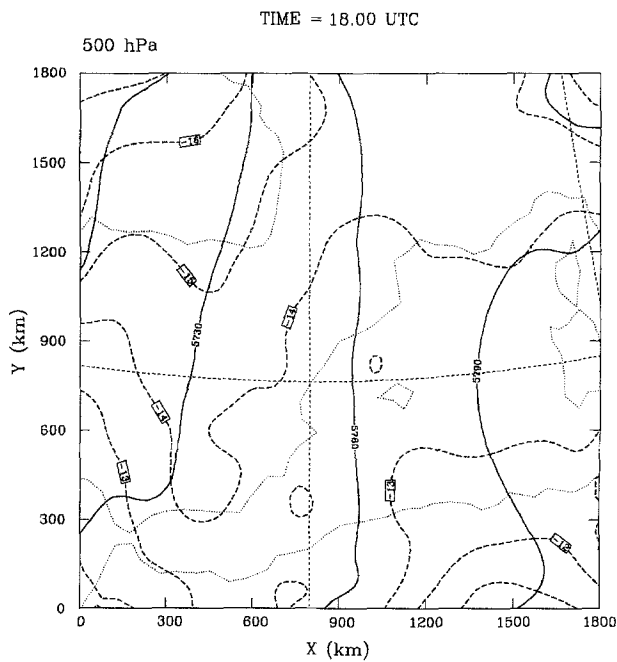
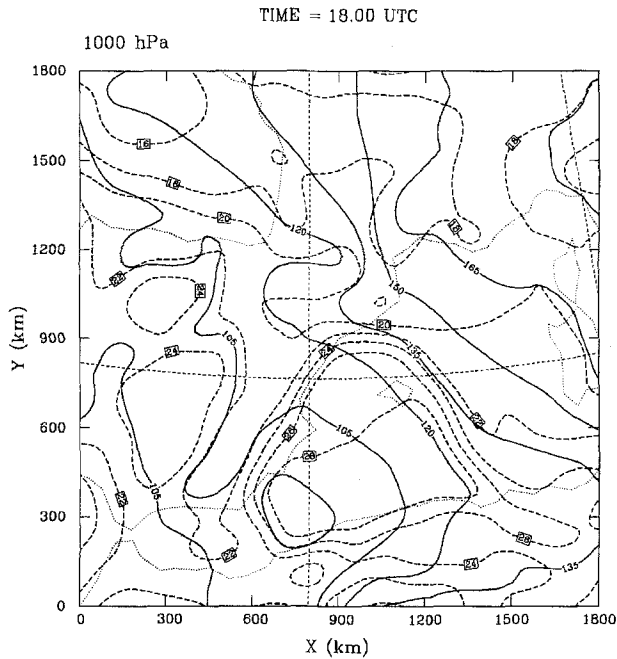


Fig. 23. Forecast fields at 18 UTC 10 October 1994, showing height (gpm, continuous line) and temperature (°C, dashed line): (a) 1000 hPa, (b) 500 hPa

forecast by the model from central Valencia to northern Catalonia. Quantitatively, this forecast is also better than for the previous day, since a large area exceeding 60 mm, with peak values of 100 mm, is obtained in Catalonia. In this case, the forecast total rainfall is also essentially

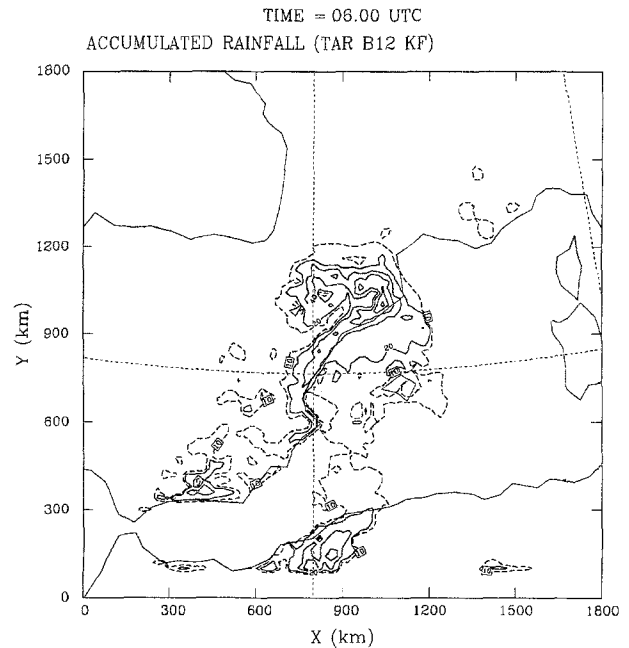


Fig. 24. Forecast total precipitation from 06 UTC 10 October 1994 to 06 UTC 11 October 1994. Contour interval is 20 mm starting at 20 mm (continuous line). Dashed contour represents 10 mm

convective. In agreement with the observed evolution of the episode, the major part of the rainfall is forecast during the first half of the day.

The main physical arguments derived for 9 October also apply for 10 October. When considering the basic simulation f_0 , less than 10 mm are given by the model in all the area of interest, including sea zones. This means that the considered factors should be fundamental for the rainfall distribution and amounts. The isolated effect of the topography on the accumulated rainfall results very important (Fig. 25a). This effect practically explains the forecast rainfall in all zones except in coastal Catalonia and over the sea (compare with Fig. 24). The effect on the 1000 hPa geopotential field at 18 UTC is shown in Fig. 25b. Comparing with Fig. 21a, it is deduced that the orographic effect, both by Atlas and by Pyrenees, is not so marked at this time. This can be attributed to the weakening of the southerly flux at upper levels.

The effect of the evaporation from the sea on the rainfall is essentially positive and helps to explain the rainfall structure depicted in Fig. 29a over the sea, south of the Balearic Islands. Only very weak actions on the low-level flow and geopotential can be attributed to the evaporation.

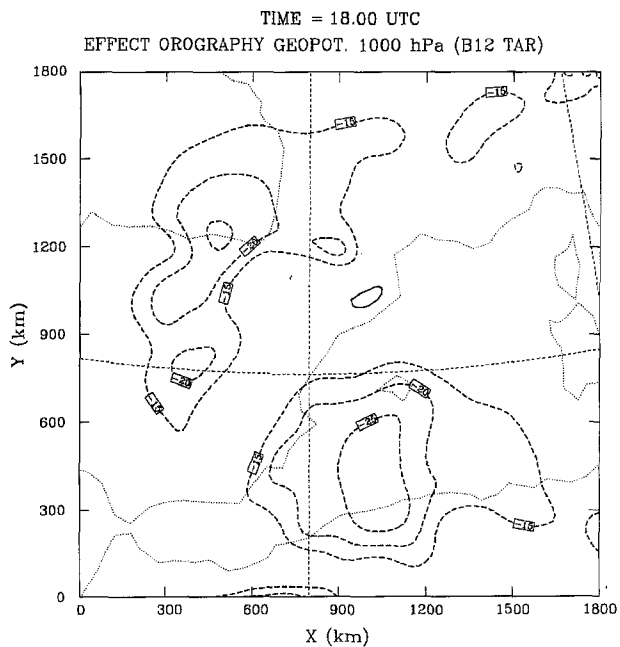
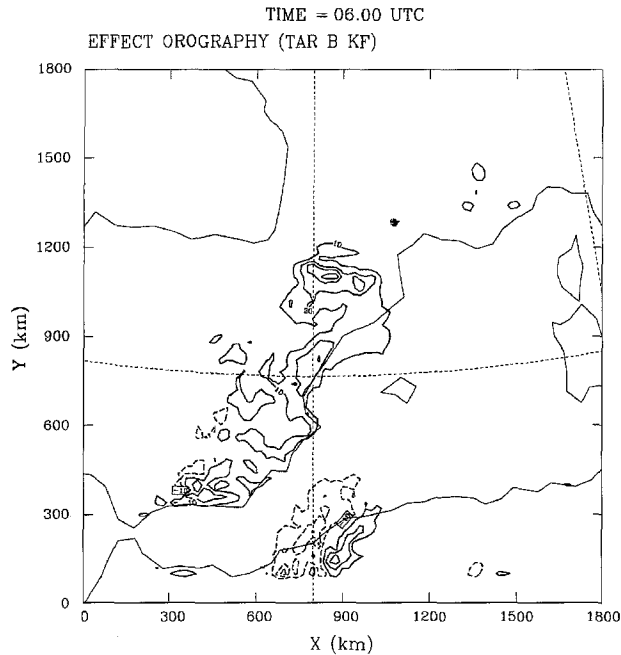
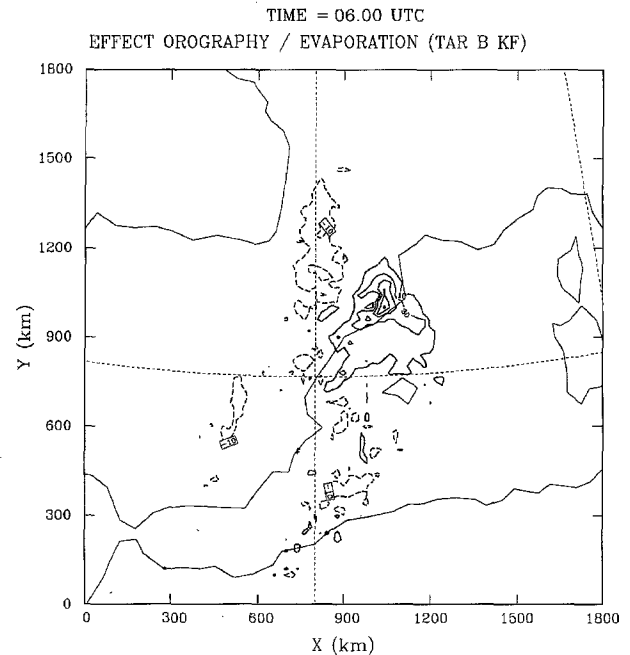


Fig. 25. Effect of the orography: (a) on the total precipitation at the end of the simulation (06 UTC 11 October 1994) (contour interval is 20 mm starting at 10 mm, continuous line, and at -10 mm, dashed line); (b) on the geopotential field at 1000 hPa (in gpm) on 18 UTC 10 October 1994

This effect becomes once again the weakest one of the three and it is not shown.

The effect of the interaction orography/evaporation turns to be the most important for



a Fig. 26. Effect of the interaction orography/evaporation on the total precipitation at the end of the simulation (06 UTC 11 October 1994) (contour interval is 20 mm starting at 10 mm, continuous line, and at -10 mm, dashed line)

explaining the rainfall north of the Balearic Islands and in particular the coastal maxima of Catalonia (Fig. 26). Correspondingly, its action is suppressive downstream over interior lands. The great importance of the synergistic effect over coastal Catalonia can be attributed to the model initial conditions of wind and relative humidity at low levels. Both fields (not shown) indicate that the flux impinging over Catalonia during the first hours of simulation must be “dry” unless evaporation from the sea is allowed. The evaporation increases the relative humidity of the air parcels flowing over the Mediterranean and the coastal mountains of Catalonia are able to develop convection. The interaction effect on the surface wind field is only remarkable over the sea close to the Catalonia coast. It acts in the sense of favouring the upslope flow, since blocking is less strong for humid air than for dry air.

5. Conclusions

The meteorological situation in which a torrential rainfall event occurred in Catalonia has been presented. At low levels, it was characterized by an anticyclone over Europe and a trough over the Algerian coast which combined to produce warm

and humid easterly flux impinging over the coastal orography of eastern Spain. At upper levels there was a synoptic wave with a trough to the southwest of Spain and a negatively tilted ridge over the western Mediterranean. A thermal ridge was also present over eastern Spain and the western Mediterranean. Meteosat images show that the development of the convective systems producing the heaviest precipitation occurred in the rear of the ridge axis and far from the trough. The convection developed over the Valencia area and then moved northeastwards along the Spanish coast, remaining stationary during several hours over south Catalonia.

A diagnostic study at synoptic scale, using ECMWF data, reveals the presence over eastern Spain and the western Mediterranean of enough ingredients for the development and maintenance of convection able to produce heavy rain. Composite charts including quasi-geostrophic upward forcing at 850 hPa, convergence of water vapour between 1000 and 850 hPa, and convective instability between 1000 and 500 hPa show that these ingredients overlapped over eastern Spain. The overlapping areas represent the zones where subsynoptic mechanisms may be more effective for the trigger of convective cells. The analysis of the available radiosonde data close to the area of interest show that the results obtained from the ECMWF data are quite representative of the actual environment. The radiosoundings also show that there was high humidity in all the troposphere, representing a favourable environment for precipitation efficiency. The comparison between the radiosonde data from Palma (Balearic Islands) and Zaragoza (inland Spain) demonstrates that the air mass over the Mediterranean is representative of the environment in which convection developed, and that it is clearly separated from the much more stable air mass of inland Spain.

Subsynoptic analyses using all the available surface and upper air data and Meteosat images, demonstrate the strong influence of the orography on the pressure and wind distributions. In particular, the Atlas range develops a shallow low over the south of the western Mediterranean and the Pyrenees causes a pressure dipole with the mesohigh over Catalonia. Both pressure anomalies combine to focalize and intensify the low level moist flux towards the Spanish coast, where

the orography provides lifting to the humid parcels. The interaction of the easterly flux with the outflow boundary of the Pyrenean mesohigh can explain the stationarity of the convection when it reached south Catalonia. A secondary weak trough identified on the 500 hPa maps, which translated between the trough and the ridge axes, could have helped the low levels lifting mechanisms to trigger the convection.

The meteorological scenario of the event resembles, in many aspects, the scenario described by Maddox et al. (1979) as the “mesohigh event” for flash floods in USA. However, the mesolow and mesohigh that interact to develop stationary convection have, in our case, an orographic origin.

The performed numerical simulations of the event have shown that the used mesoscale model is able to capture reasonably well the spatial details of the precipitation field. However, quantitative precipitation forecast is worse, since the recorded maxima are underestimated. The forecast geopotential and temperature fields at low levels display a low pressure area over the Algerian coast, a pressure dipole about the Pyrenees, and a warm air tongue extending from Africa towards the Spanish coast. Such structures are supported by the subjective sub-synoptic analysis and have been associated with the important Atlas and Pyrenees orographic systems.

In order to get a better understanding of some physical mechanisms acting in this kind of torrential events, we have investigated the effects of the orography and the evaporation from the sea following the methodology of Stein and Alpert (1993). Both factors have been traditionally considered as the most important for the development of heavy rain in eastern Spain (Miró-Granada, 1974). Results of the factor separation study show:

a) The orography is responsible for the development of the shallow low in the lee of the Atlas over the Algerian coast, as well as for the pressure dipole about the Pyrenees. These structures, which are more noticeable when the upper levels flow is strong, lead to an intensification of the pressure gradient over the western Mediterranean and therefore to an enhancement of the easterly flux towards the Spanish coasts. In addition, the orography is also responsible for the warm air anomaly present at low levels over the

south of the western Mediterranean. This warm air tongue and the easterly flux combine to reinforce the warm advection towards the Spanish coastal orography.

b) The evaporation from the sea does not produce, when orography is not present, any remarkable effect on the precipitation, geopotential and wind fields.

c) The combined effect of the orography and the evaporation was the most decisive for the spatial distribution of the rainfall in the studied event. In particular, it is responsible for the coastal maxima located in northern Valencia (9 October) and Catalonia (10 October). In previous studies (Romero et al., 1997; Romero et al., 1998b) the combined effect was not so relevant because the air mass advected towards the coastal area was already charged of enough moisture. However, our result illustrates the great importance that latent heat fluxes during the course of the simulation may have in other cases, and suggests that quantitative precipitation forecasts in the western Mediterranean area may be especially sensitive to sea surface temperature.

Acknowledgements

This work was supported by DGICYT PB94-1169-CO2-2 grant. The authors acknowledge Prof. J. L. Casanovas of the University of Valladolid (Spain) for providing the Meteosat images of the event. Precipitation data were provided by the Spanish Instituto Nacional de Meteorología (INM).

References

- Alarcón, M., 1993: *Simulation of Long-range Atmospheric Transport and Deposition of Substances at the Western Mediterranean: Trajectory Models and Diffusion-Deposition Processes*. Ph. D. Thesis. Universitat de Barcelona, 179 pp.
- Bessemoulin, P., Bougeault, P., Genovés, A., Jansá, A., Puech, D., 1993: Mountain pressure drag during PYREX. *Beitr. Phys. Atmos.*, **66**, 305–325.
- Codina, B., Aran, M., Young, S., Redaño, A., 1997: Prediction of a mesoscale convective system over Catalonia (northeastern Spain) with a nested numerical model. *Meteorol. Atmos. Phys.*, **62**, 9–22.
- Davies-Jones, R., Burgess, D., Foster, M., 1990: *Test of Helicity as a Tornado Forecast Parameter*. 16th Conference on Severe Local Storms, Amer. Meteor. Soc., 588–592.
- Doswell, C. A., 1987: The distinction between large-scale and mesoscale contribution to severe convection: A case study example. *Wea. Forecasting*, **2**, 3–16.
- Doswell, C. A. III, Ramis, C., Romero, R., Alonso, S., 1998: A diagnostic study of three heavy precipitation episodes in the western Mediterranean region. *Wea. Forecasting*, **13**, 102–124.
- Duquet, R. T., 1964: *Data Processing for Isentropic Analysis*, Tech. Rep. num. 1, contract (30-1)–3317, Air Force Cambridge Research Laboratories, Hanscom AFB, MA 01731.
- Emanuel, K. A., 1983: On assessing local conditional symmetric instability from atmospheric soundings. *Mon. Wea. Rev.*, **111**, 2016–2033.
- Endlich, R. M., 1967: An iterative method for altering the kinematic properties of wind fields. *J. Appl. Meteor.*, **6**, 837–844.
- Farrel, R. J., Carlson, T. N., 1989: Evidence for the role of the Lid and Underrunning in an outbreak of tornadic thunderstorms. *Mon. Wea. Rev.*, **117**, 857–871.
- Fernández, C., Gaertner, M. A., Gallardo, C., Castro, M., 1995: Simulation of a long-lived meso- β scale convective system over the Mediterranean coast of Spain. Part I: Numerical predictability. *Meteorol. Atmos. Phys.*, **56**, 157–179.
- Font, I., 1983: *Climatología de España y Portugal*. Instituto Nacional de Meteorología, Apartado 285, 28071, Madrid, 296 pp.
- García-Dana, F., Font, R., Rivera, A., 1982: *Meteorological Situation During the Heavy Rain Event in the Eastern Zone of Spain During October-82*. Madrid: Instituto Nacional de Meteorología.
- Hakim, G. J., Uccellini, L. W., 1992: Diagnosing coupled Jet Streak circulations for a northern plains snow band from the operational nested-grid model. *Wea. Forecasting*, **7**, 26–48.
- Hoskins, B. J., Pedder, M. A., 1980: The diagnosis of middle latitude synoptic development. *Quart. J. Roy. Meteor. Soc.*, **106**, 707–719.
- Kain, J. S., Fritsch, J. M., 1990: A one-dimensional entraining/detraining plume model and its application in convective parameterization. *J. Atmos. Sci.*, **47**, 2784–2802.
- Llasat, M. C., 1987: *Heavy Rain Events in Catalonia: Genesis, Evolution and Mechanism*. (In Spanish), Ph. D. Thesis., Univ. of Barcelona Press, 250 pp.
- Maddox, R. A., Chappell, C. F., Hoxit, L. R., 1979: Synoptic and meso- α scale aspects of flash flood events. *Bull. Amer. Meteor. Soc.*, **60**, 115–123.
- Miró-Granada, J., 1974: Les crues catastrophiques sur le Méditerranée occidentale. *AMS-AISH Public.*, **12**, 119–132.
- Nickerson, E. C., Richard, E., Rosset, R., Smith, D. R., 1986: The numerical simulation of clouds, rain and airflow over the Vosges and Black forest mountain: a meso- β model with parameterized microphysics. *Mon. Wea. Rev.*, **114**, 398–414.
- Pinty, J. P., 1984: *Une méthode variationnelle d'ajustement des champs de masse et de vent*, Note 72 de l'I. O. P. G., Université de Clermont II.
- Ramis, C., Llasat, M. C., Genovés, A., Jansá, A., 1994: The October-1987 floods in Catalonia: Synoptic and Mesoscale Mechanisms. *Meteor. Applicat.*, **1**, 337–350.

- Ramis, C., Alonso, S., Llasat, M. C., 1995: A comparative study of two cases of heavy rain in Catalonia, *Surv. in Geophys.*, **16**, 141–161.
- Riosalido, R., 1990: *Characterization of mesoscale convective systems by satellite pictures during PREVI-MET MEDITERRANEO-89*, (in Spanish). Segundo Simposio Nacional de Predicción. Instituto Nacional de Meteorología, Apartado 285, 28071, Madrid, 135–148.
- Rockwood, A. A., Maddox, R. A., 1998: Mesoscale and synoptic interactions leading to intense convection: the case of 7 June 1982. *Wea. Forecasting*, **3**, 51–68.
- Romero, R., Ramis, C., Alonso, S., 1997: Numerical simulation of an extreme rainfall event in Catalonia: Role of orography and evaporation from the sea. *Quart. J. Roy. Meteor. Soc.*, **123**, 537–559.
- Romero, R., Guijarro, J. A., Ramis, C., Alonso, S., 1998a: A 30 year (1964–1993) daily rainfall data base for the Spanish mediterranean regions: First exploratory study. *Int. J. Climatol.*, **18**, 541–560.
- Romero, R., Ramis, C., Alonso, S., Doswell III C. A., Stensrud, D. J., 1998b: Mesoscale model simulations of three heavy precipitation events in the western Mediterranean region. *Mon. Wea. Rev.*, **126**, 1859–1881.
- Schofield, R. A., Purdom, J. F. W., 1986: The use of satellite data for mesoscale analysis and forecasting applications. In: Ray, P. S. (ed.), *Mesoscale Meteorology and Forecasting*, Amer. Meteor. Soc., 118–150.
- Shapiro, R., 1970: Smoothing, filtering and boundary effects. *Rev. Geophys. Space Phys.*, **8**, 359–387.
- Stein, U., Alpert, P., 1993: Factor separation in numerical simulations. *J. Atmos. Sci.*, **50**, 2107–2115.
- Tudurí, E., Ramis, C., 1997: The environments of significant convective events in the western Mediterranean. *Wea. Forecasting*, **12**, 294–306.
- Uccellini, L. W., 1975: A case study of apparent gravity waves initiation of severe convection storms. *Mon. Wea. Rev.*, **103**, 497–513.
- Uccellini, L. W., Johnson, D. R., 1979: The coupling of upper and lower Jet Streaks and implications for the development of severe convective storms. *Mon. Wea. Rev.*, **107**, 682–703.

Authors' addresses: C. Ramis, R. Romero, V. Homar and S. Alonso, Meteorology Group, Departament de Física, Universitat de les Illes Balears, Palma de Mallorca, Spain; M. Alarcón, Departament de Física i Enginyeria Nuclear, Universitat Politècnica de Catalunya, Vilanova i la Geltrú, Barcelona, Spain.